Electronic Supplementary Material (ESI) for Dalton Transactions.

Supporting Information

Synthesis, characterization, photophysical, electrochemical properties and biomolecular interaction of 2,2′-biquinoline based phototoxic Ru(II)/Ir(II) complexes

Utpal Das, Priyankar Paira*

CHARACTERIZATION OF COMPLEXES

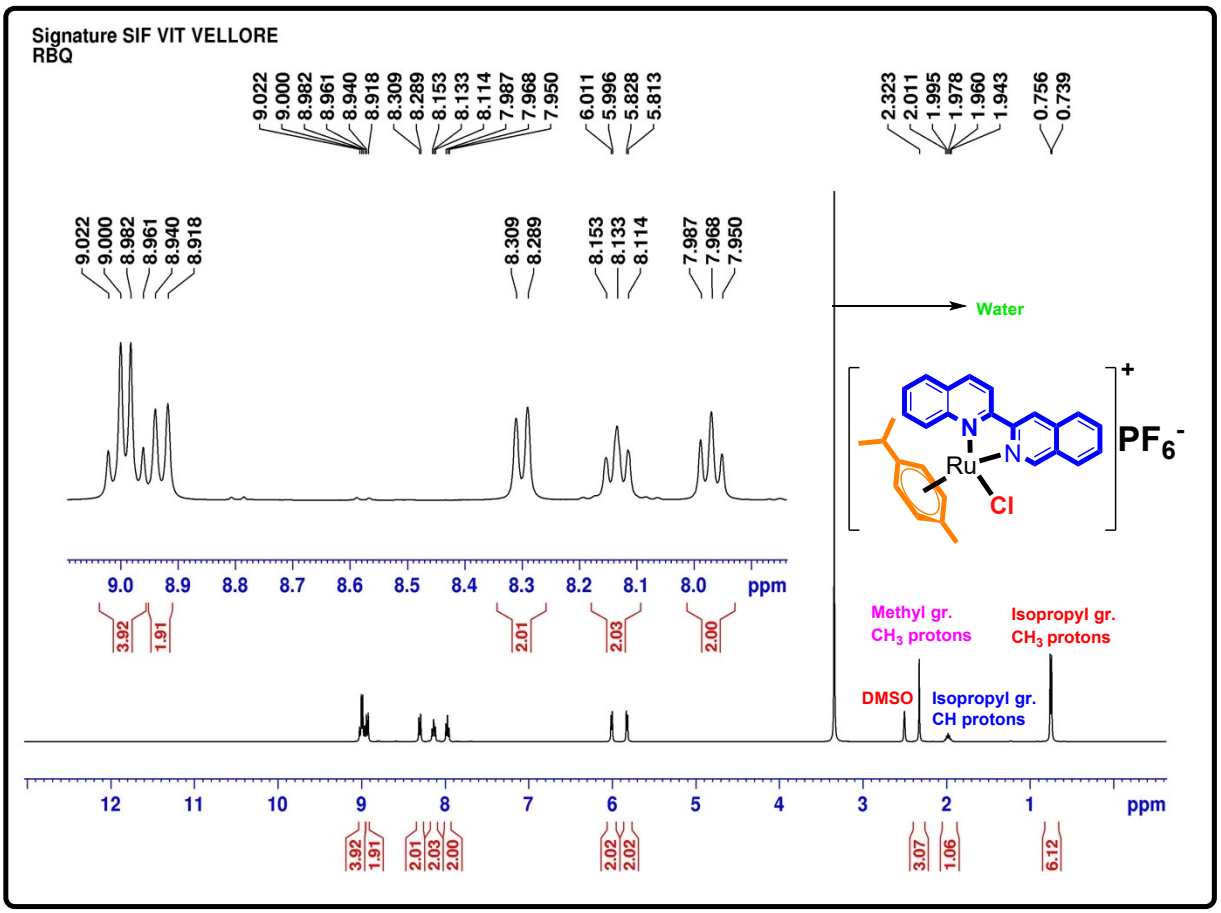

Fig. S1: ^{1}HNMR of complex RuBQ

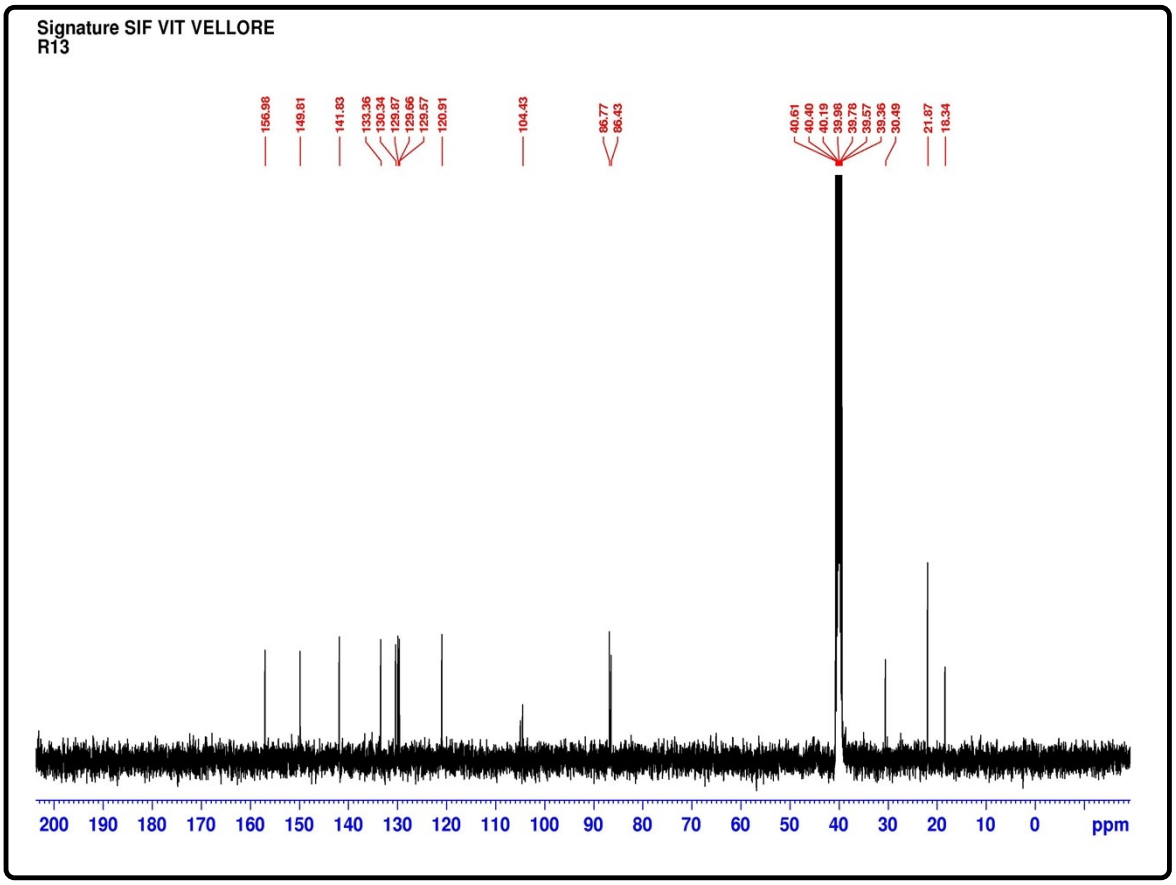

Fig. S2: ^{13}C NMR of complex RuBQ

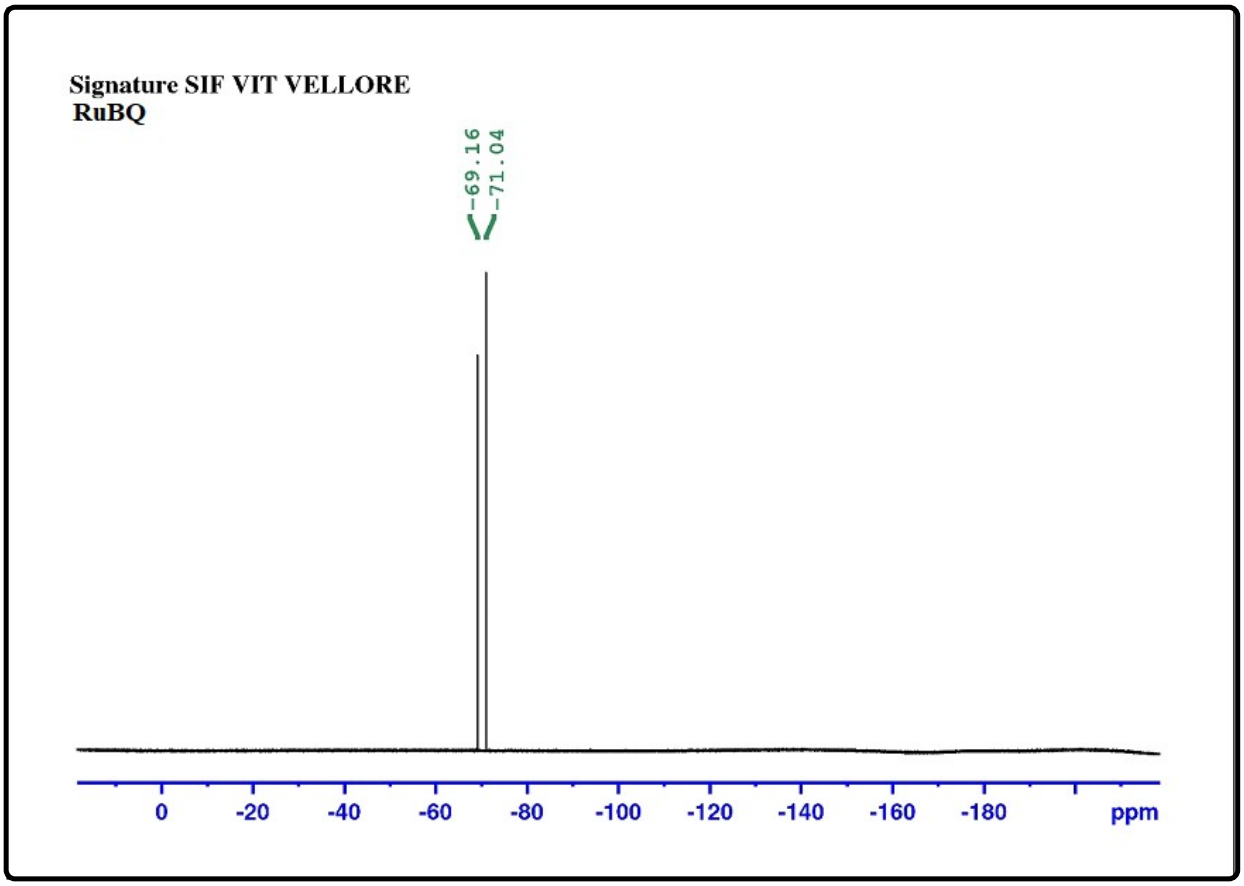

Fig. S3: ^{19}F NMR of complex RuBQ

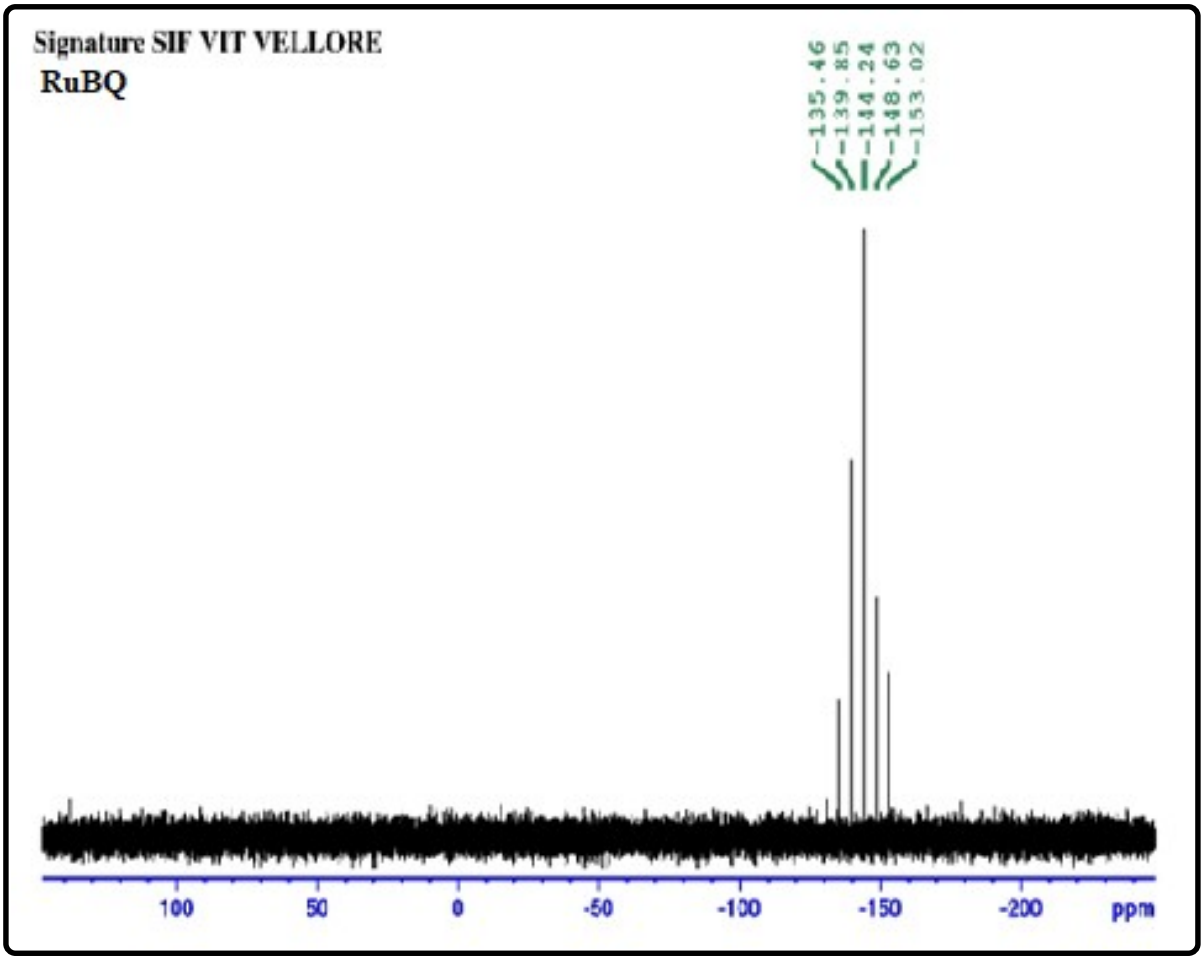

Fig. S4: ^{31}P NMR of complex RuBQ

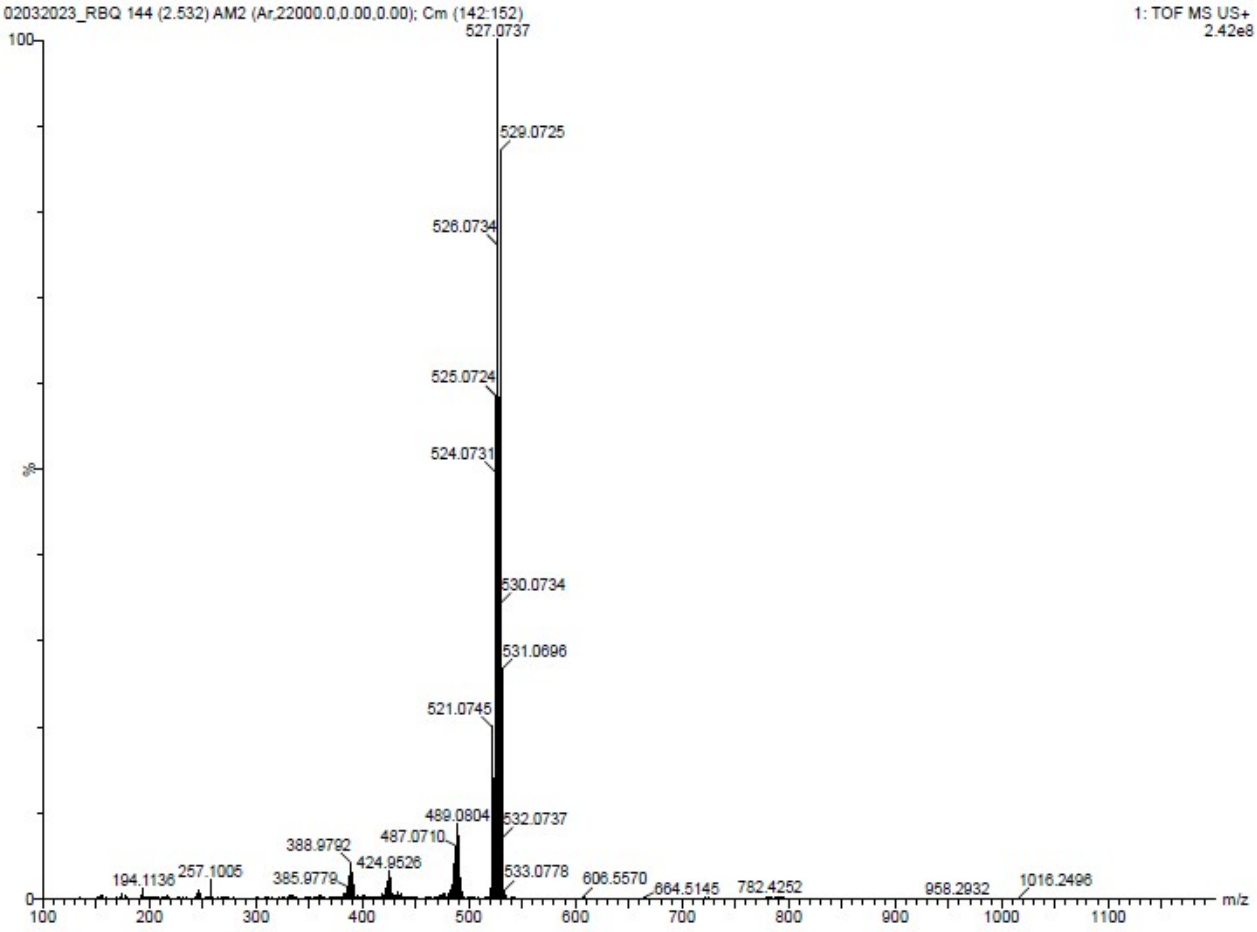
02032023_RBQ 144 (2.532) AM2 (Ar,22000.0,0.00,0.00); Cm (142:152)
1: TOF MS US+
2.42e8
100
%
0
m/z
527.0737
529.0725
526.0734
525.0724
524.0731
530.0734
531.0696
521.0745
489.0804
532.0737
487.0710
388.9792
424.9526
194.1136
257.1005
385.9779
533.0778
606.5570
664.5145
782.4252
958.2932
1016.2496
100
200
300
400
500
600
700
800
900
1000
1100

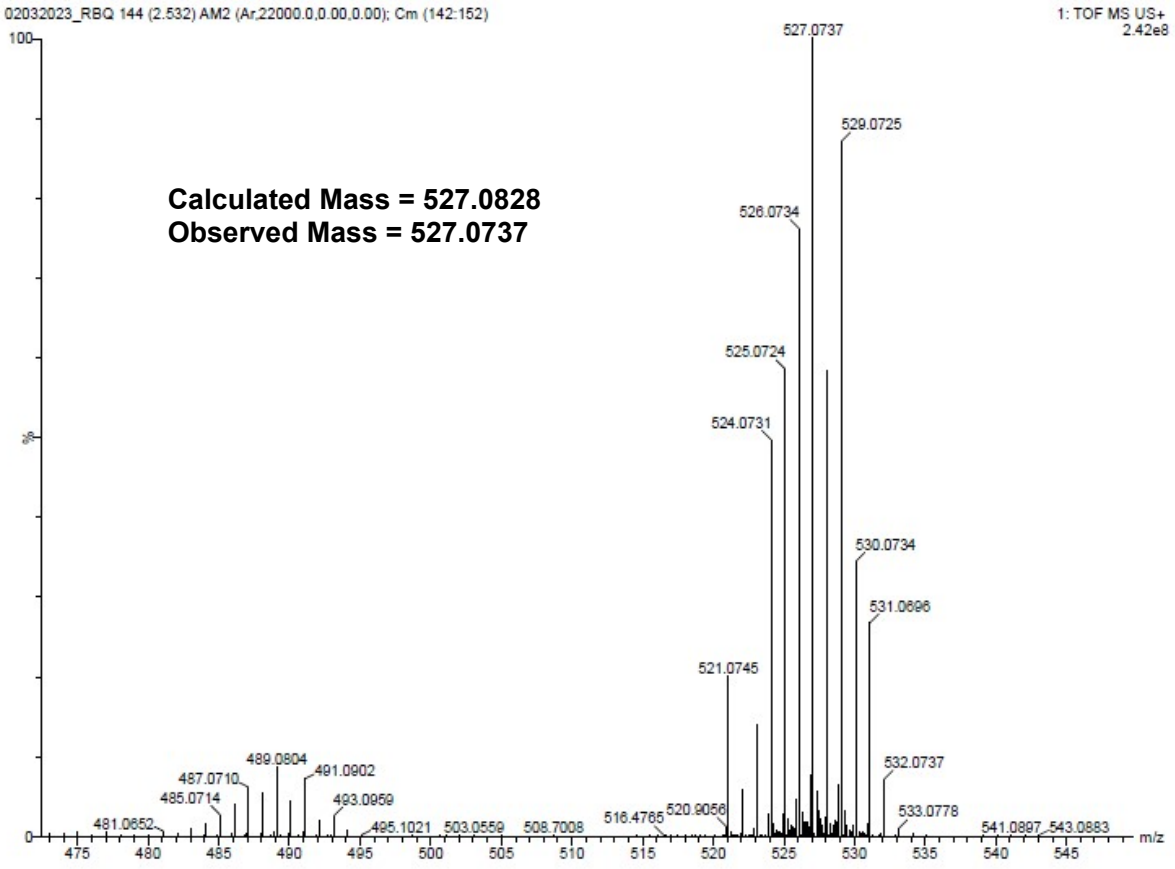

Fig. S5: ESI-HRMS spectrum of complex RuBQ

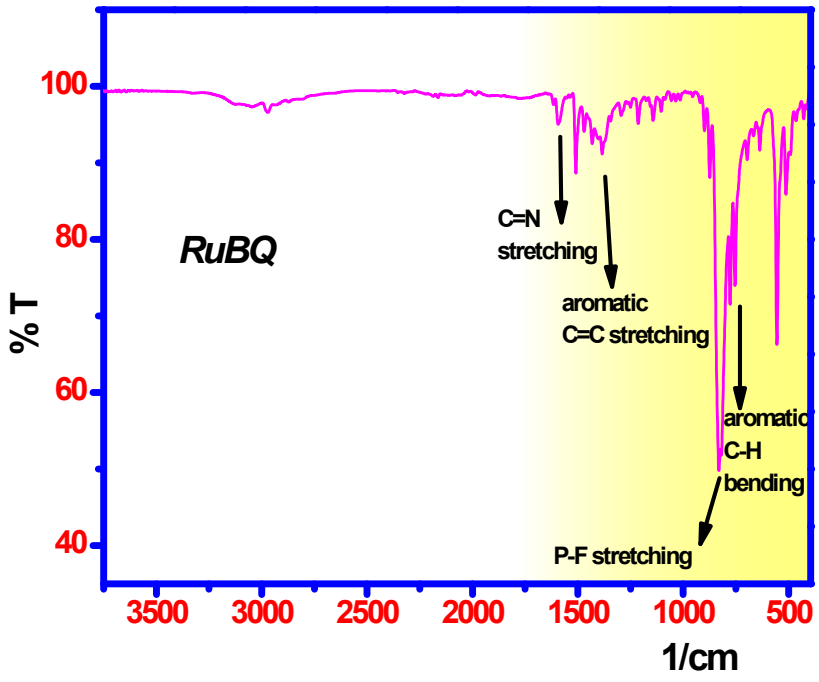

Fig. S6: IR spectrum of Complex RuBQ

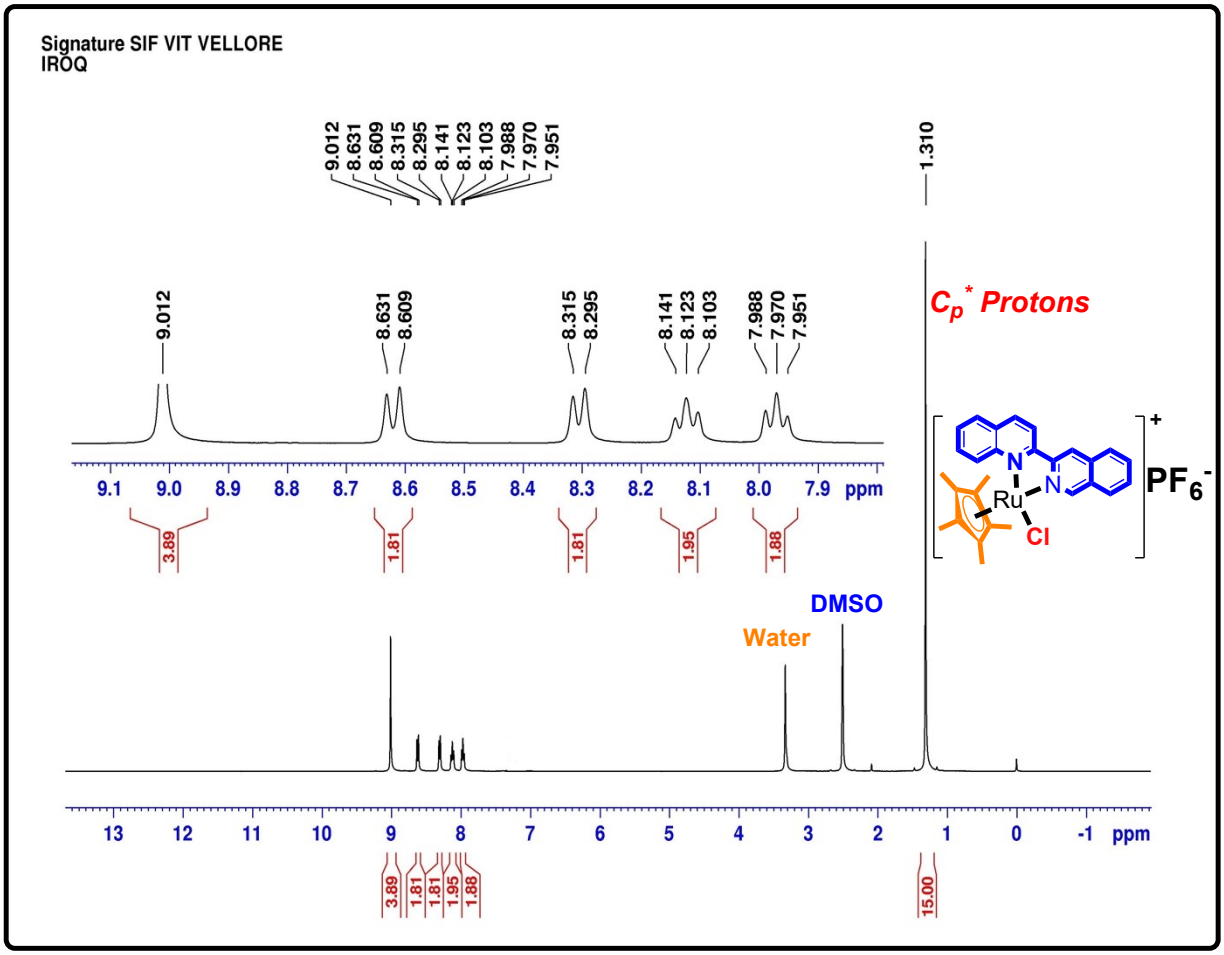

Fig. S7: ^{1}H NMR of complex IrBQ

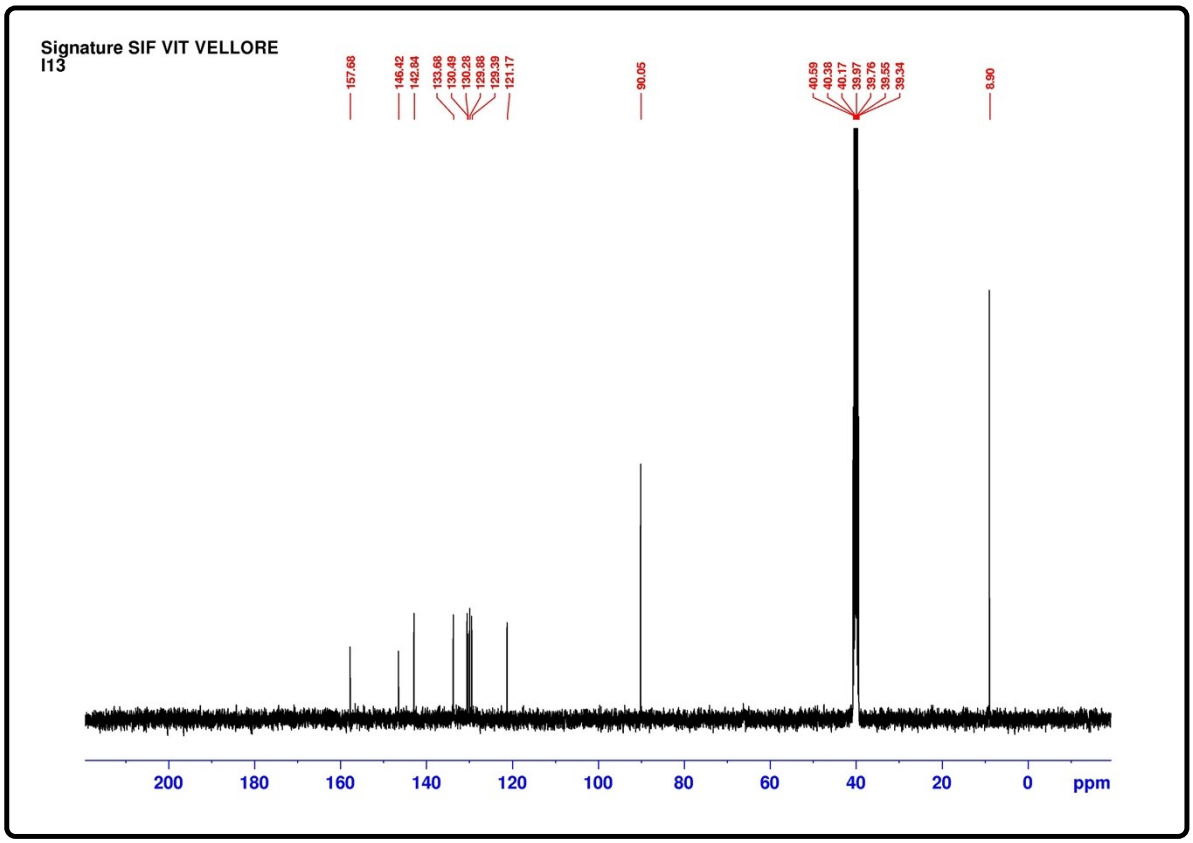

Fig. S8: ^{13}C NMR of complex IrBQ

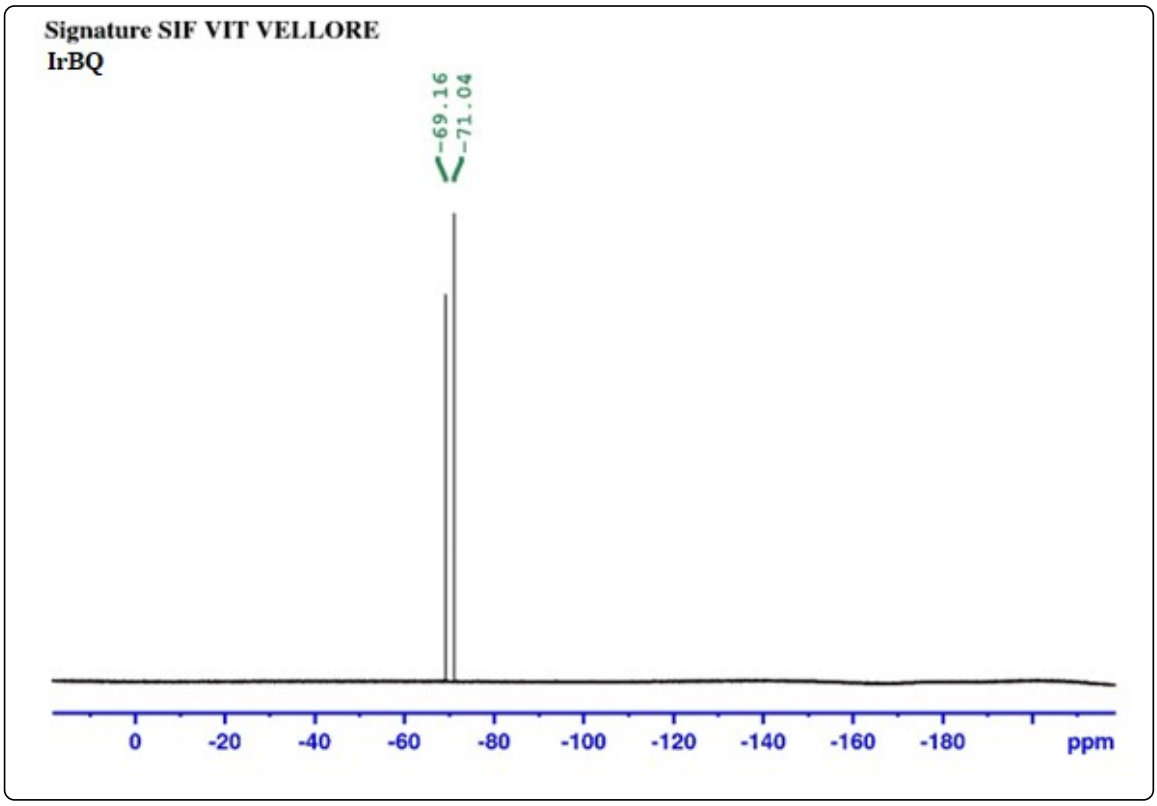

Fig. S9: ^{19}F NMR of complex IrBQ

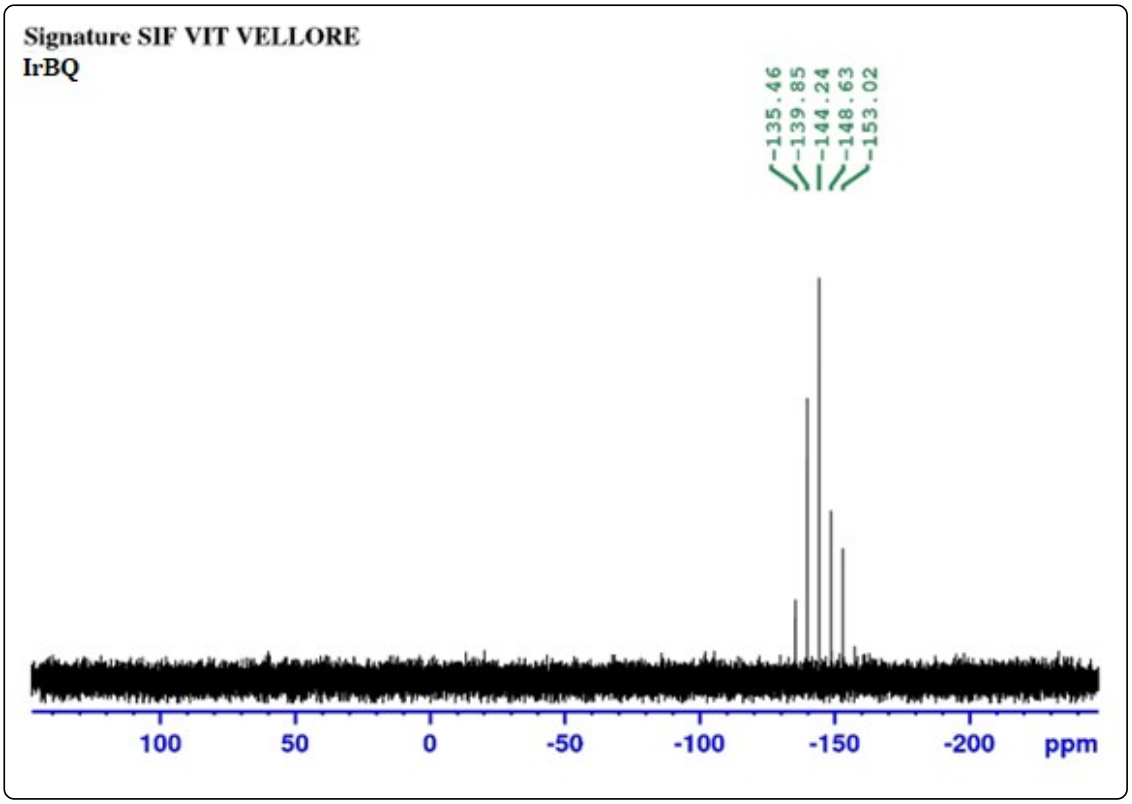

Fig. S10: ^{31}P NMR of complex IrBQ

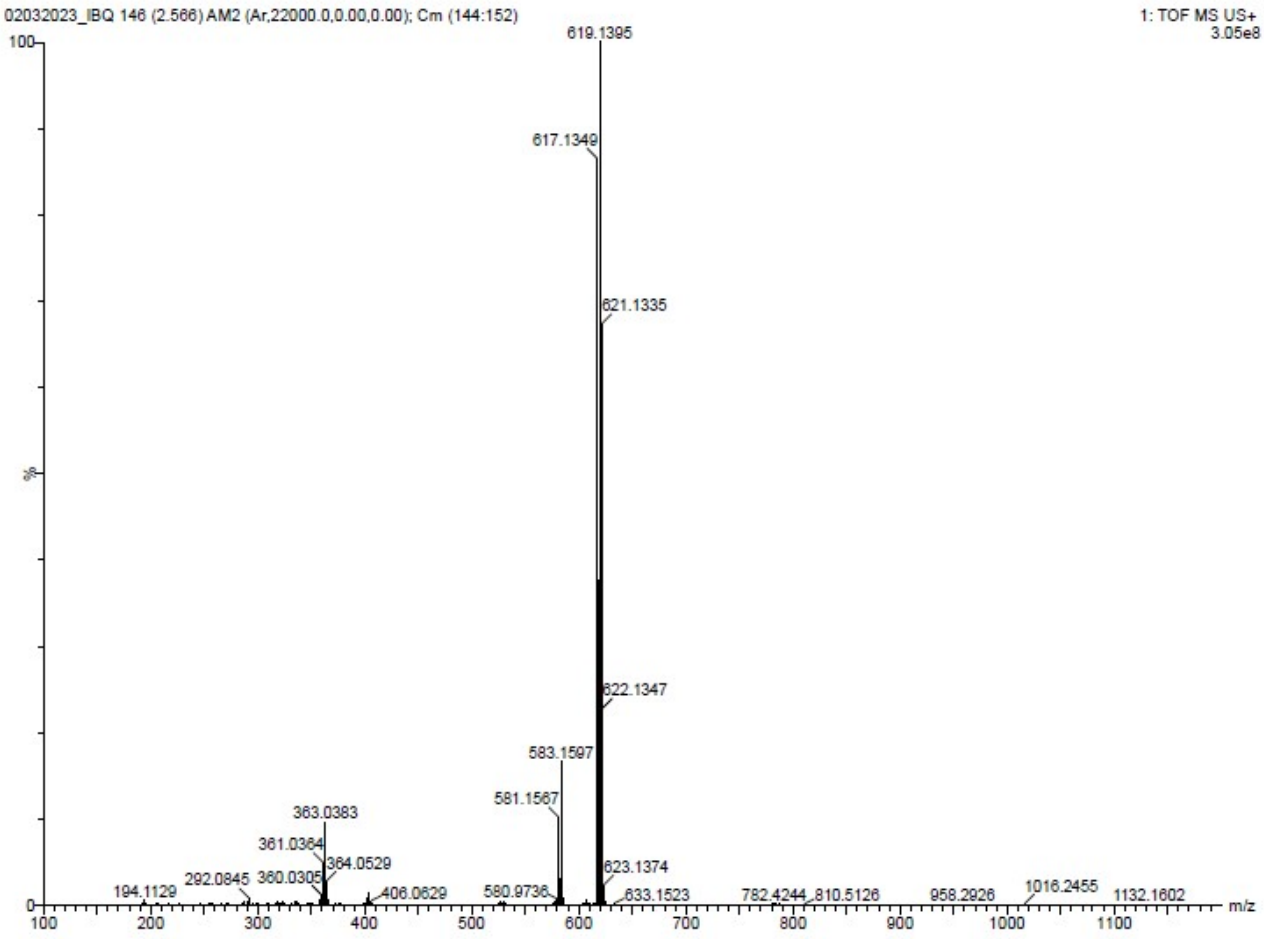
02032023_IBQ 146 (2.566) AM2 (Ar,22000.0,0.00,0.00); Cm (144:152)
1: TOF MS US+
3.05e8
100
%
0
619.1395
617.1349
621.1335
622.1347
583.1597
581.1567
363.0383
361.0364
364.0529
623.1374
194.1129
292.0845
360.0305
406.0629
580.9736
633.1523
782.4244
810.5126
958.2926
1016.2455
1132.1602
m/z
100
200
300
400
500
600
700
800
900
1000
1100

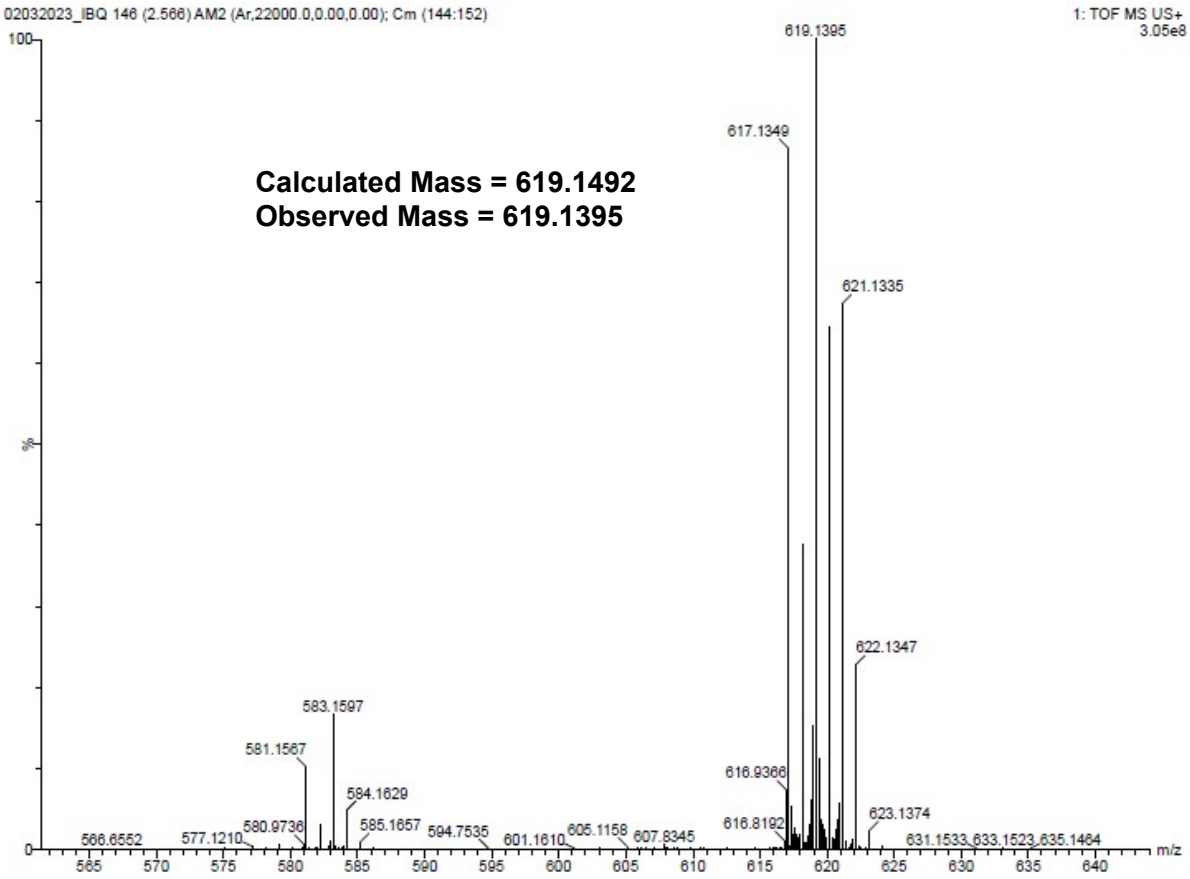

Fig. S11: ESI-HRMS spectrum of complex IrBQ

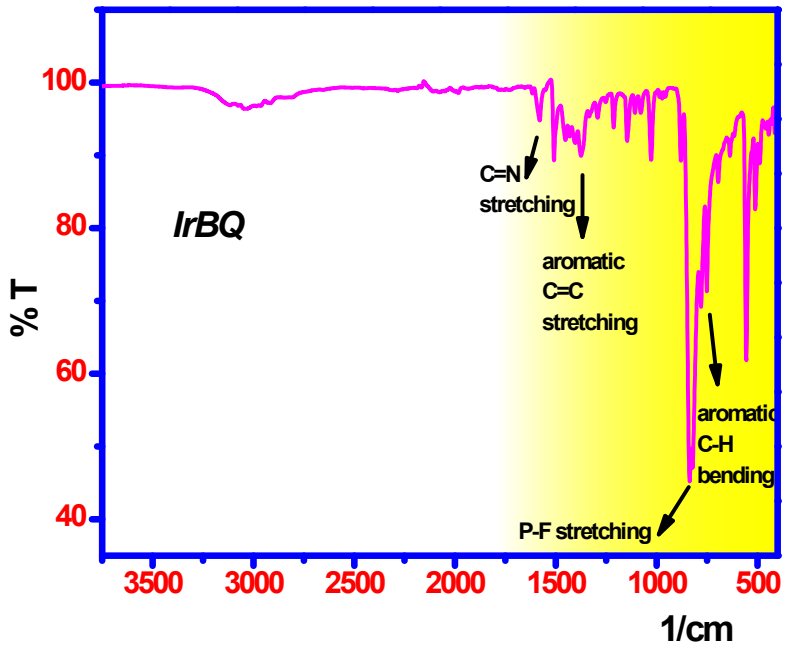

Fig. S12: IR spectrum of Complex IrBQ

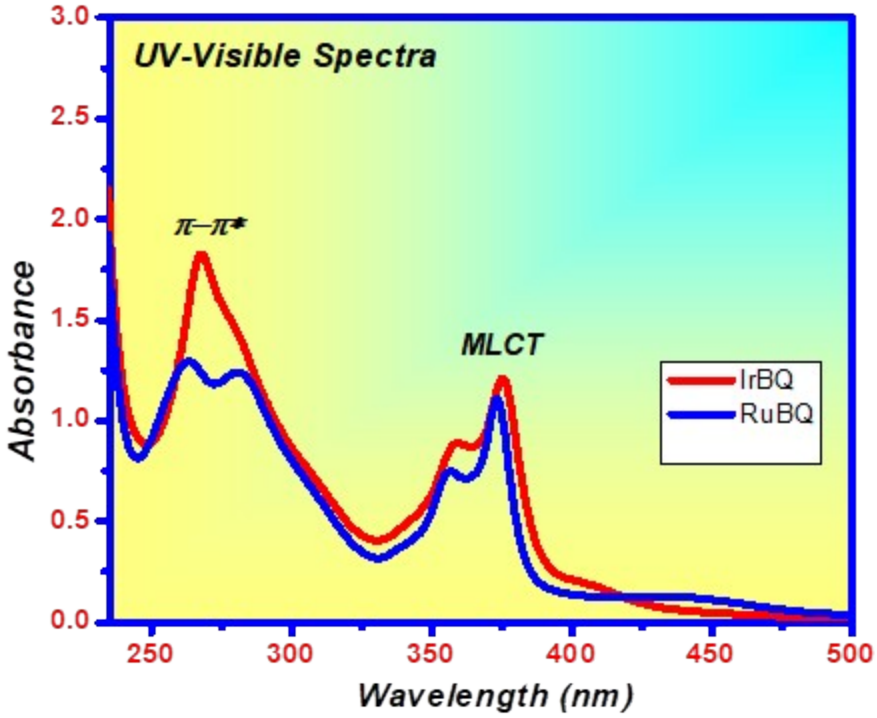

Fig. S13: UV-Vis spectra of complexes RuBQ and IrBQ with concentration of 3×10^{-5} M.

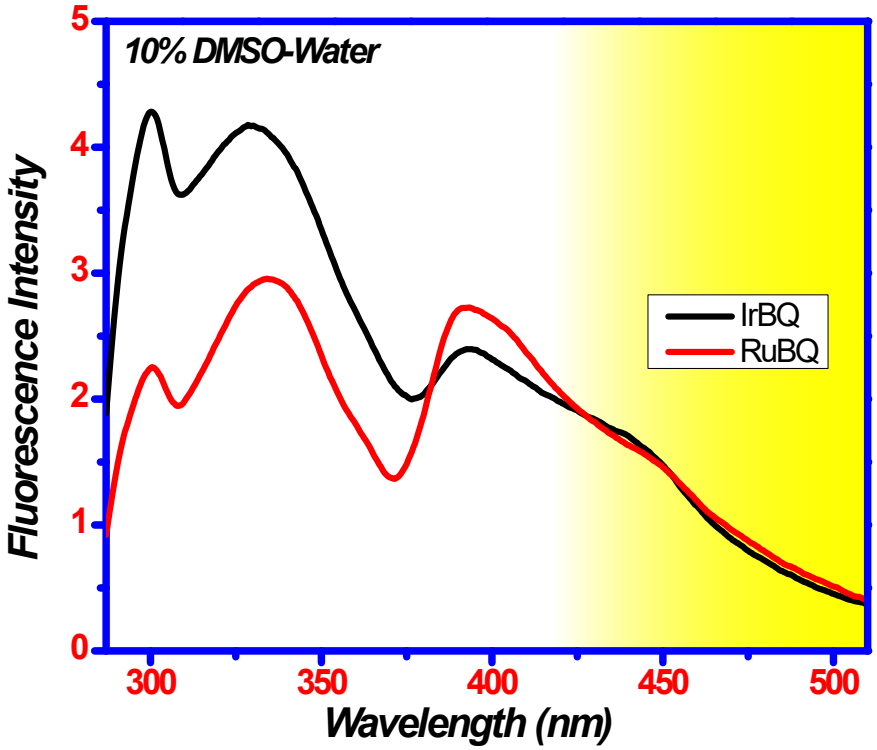

Fig. S14: Emission spectra of complexes RuBQ, and IrBQ in 10% DMSO-Water at 267 nm

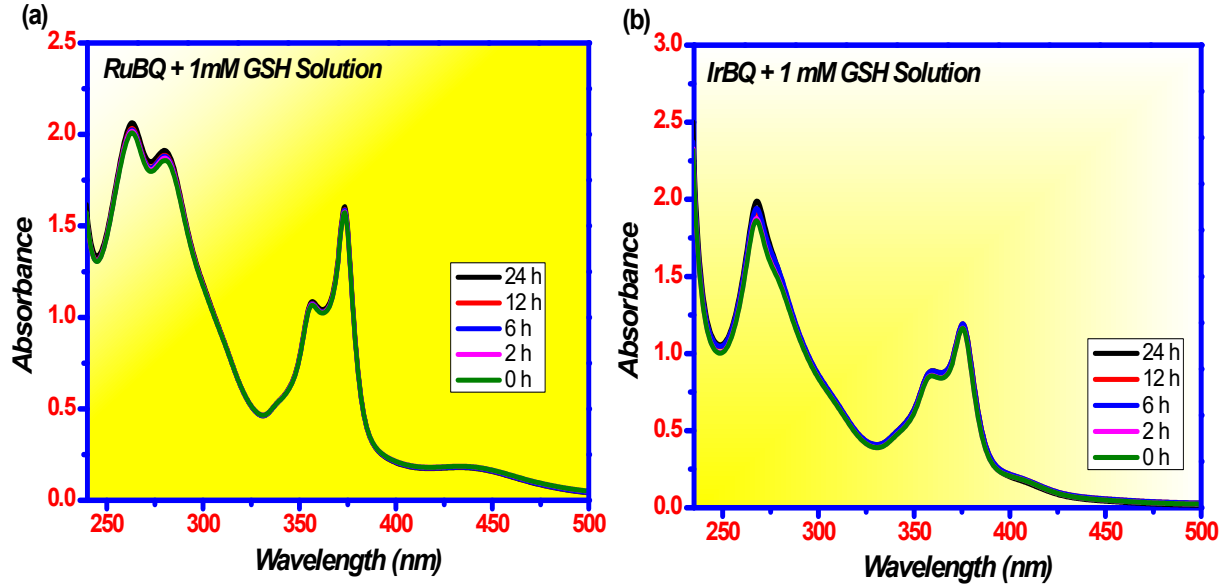

Fig. S15: Stability of the complexes RuBQ (a), and IrBQ (b) with concentration of 3×10^{-5} M in 1 mM aqueous GSH media.

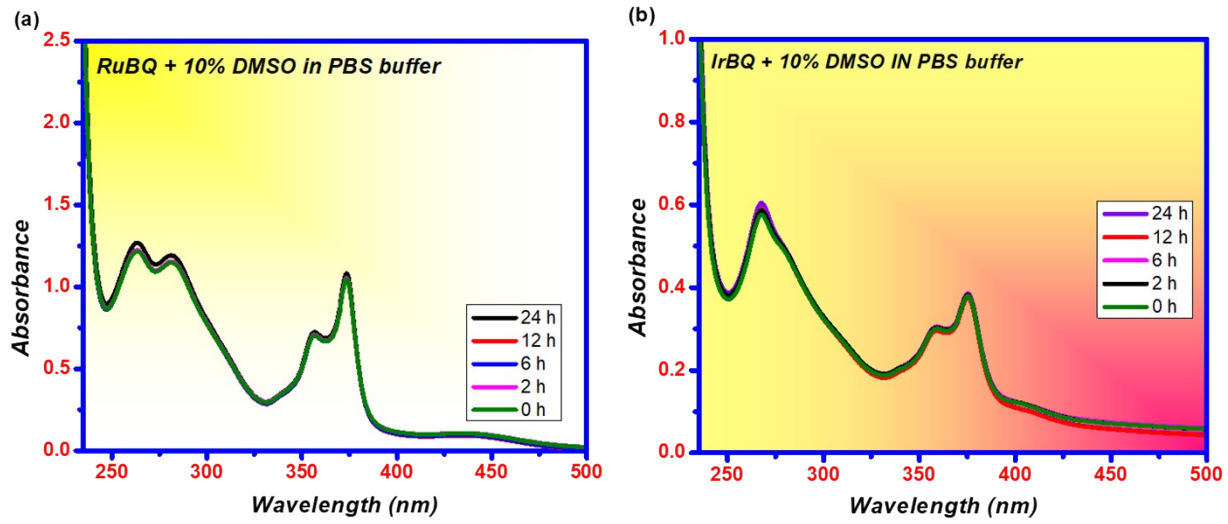

Fig. S16: Stability in 10% DMSO-PBS buffer media for complexes RuBQ (a), and IrBQ (b) with concentration of 3×10^{-5} M.

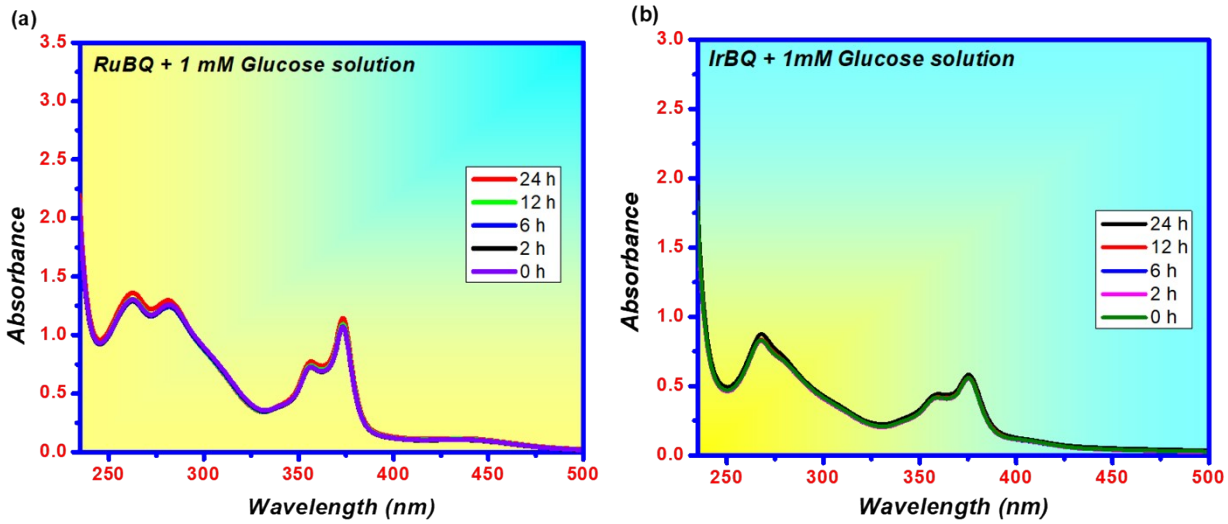

Fig. S17: Stability in 1 mM Glucose solution for complexes RuBQ (a), and IrBQ (b) with concentration of 3×10^{-5} M.

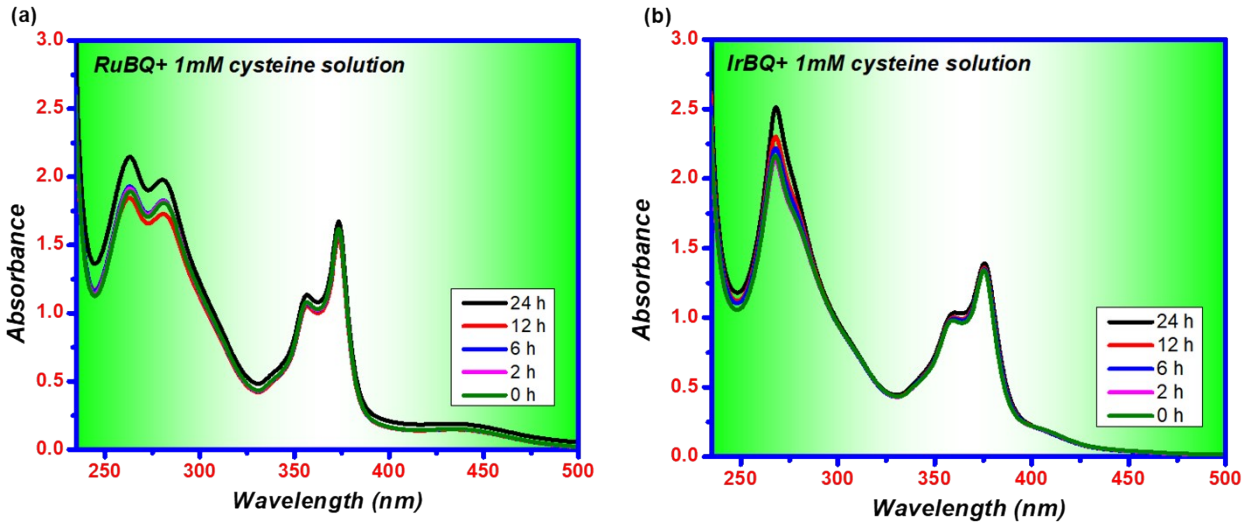

Fig. S18: Stability in 1 mM cysteine solution for complexes RuBQ (a), and IrBQ (b) with concentration of 3 × 10^{-5} M.

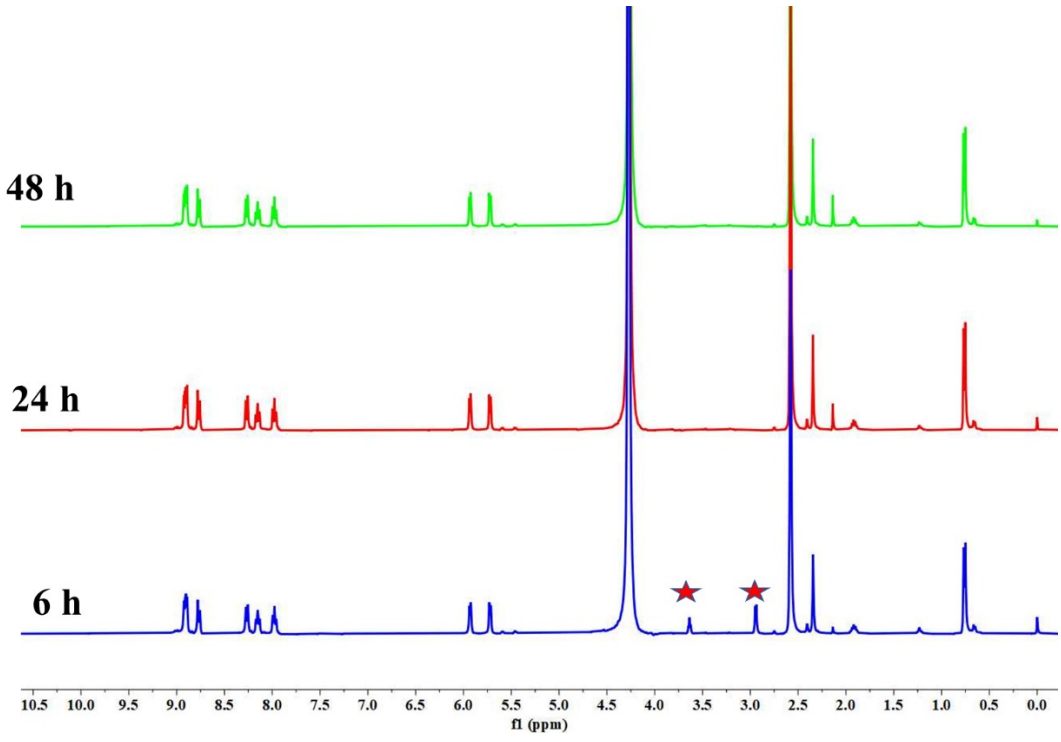

Fig. S19: Interaction of RuBQ complex with Cys molecules. ★ Peaks were vanished after 6 h.

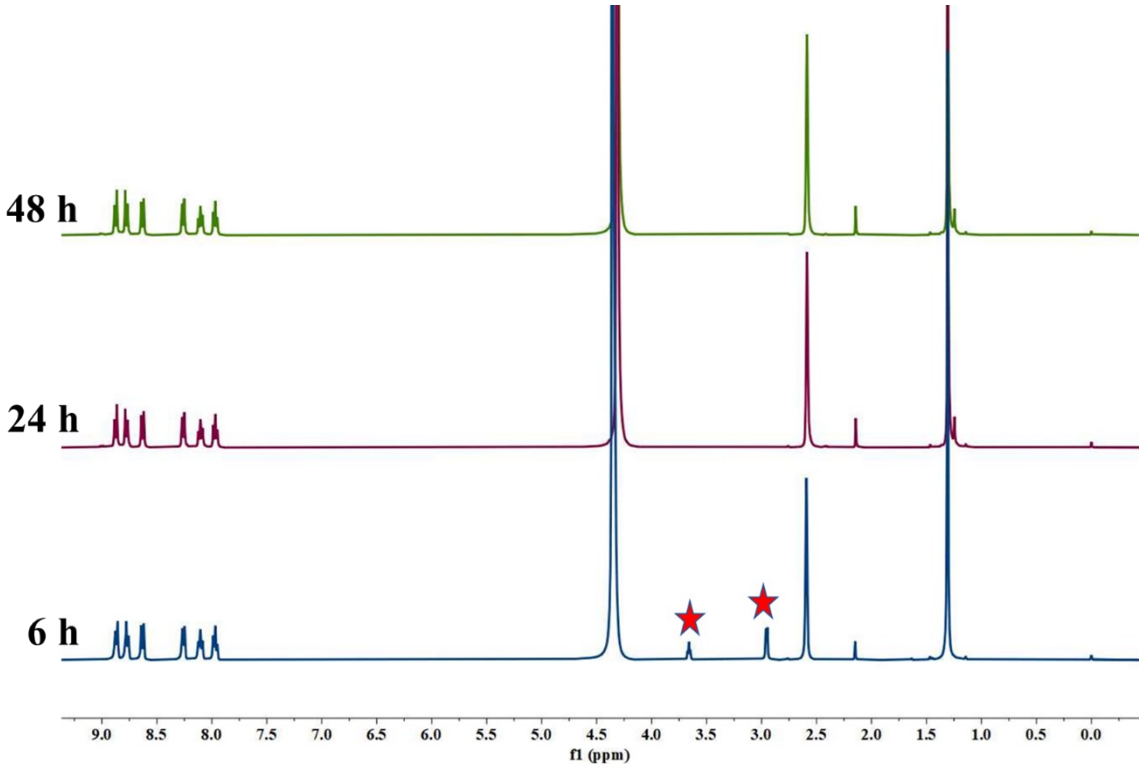

Fig. S20: Fig. S15: Interaction of IrBQ complex with Cys molecules. ★ Peaks were vanished after 6 h.

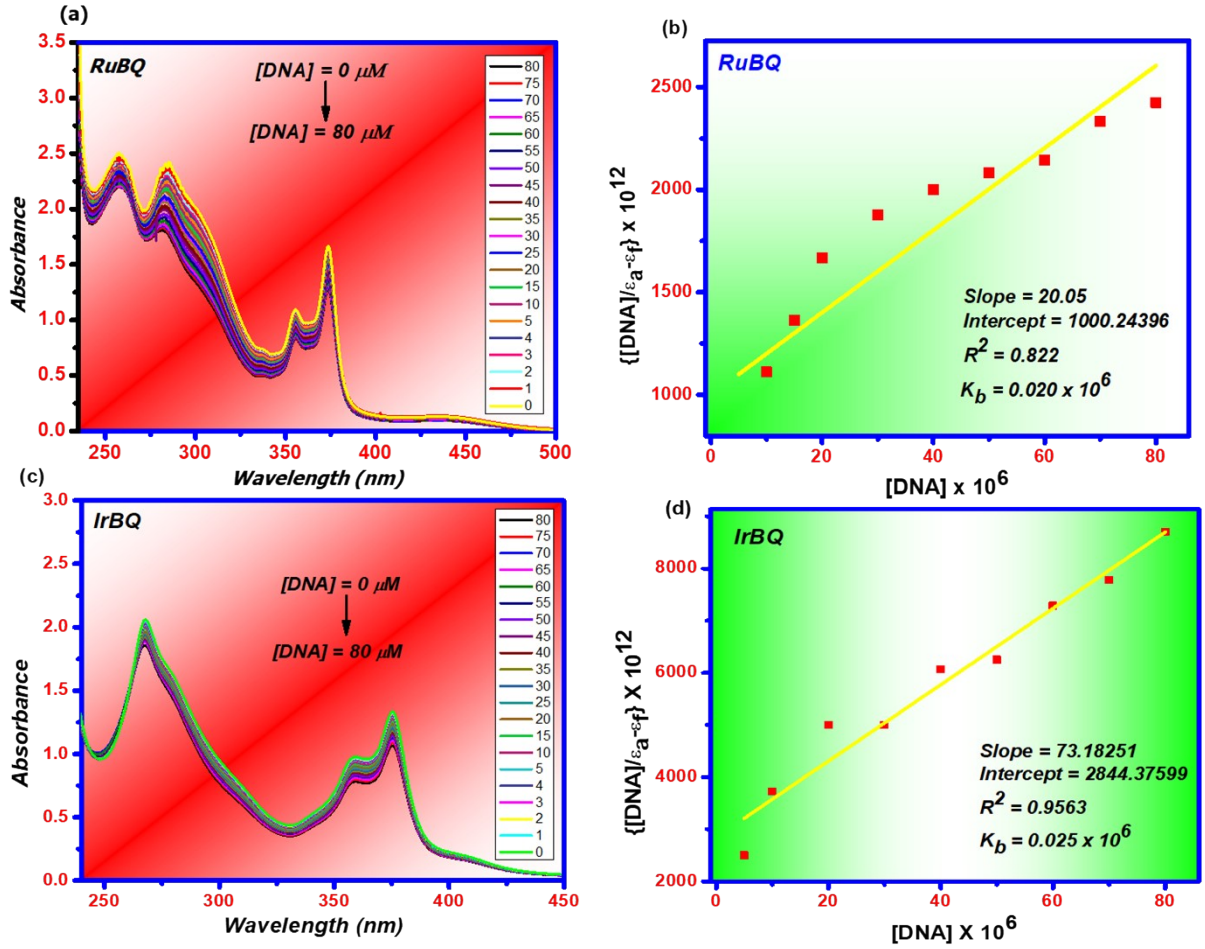

Fig. S21: DNA binding plots of all complexes RuBQ (a), and IrBQ (c). [DNA]/(ε_a-ε_f) vs. [DNA] linear plots of all complexes RuBQ (b), and IrBQ (d) with concentration of 5 × 10^{-5} M

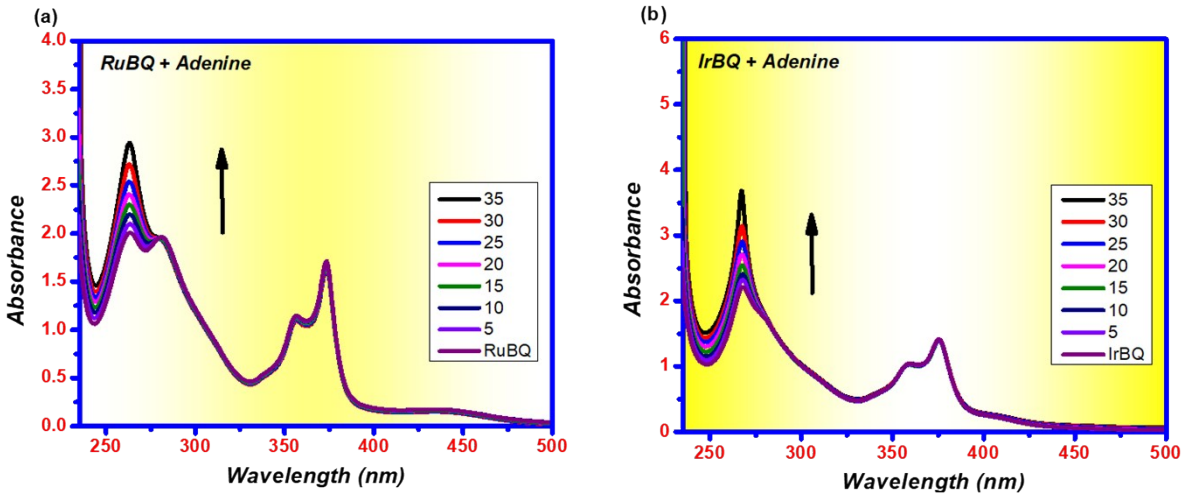

Fig. S22: Concentration dependent binding study of RuBQ and IrBQ complexes with concentration of 3 × 10^{-5} M with 1 mM Adenine.

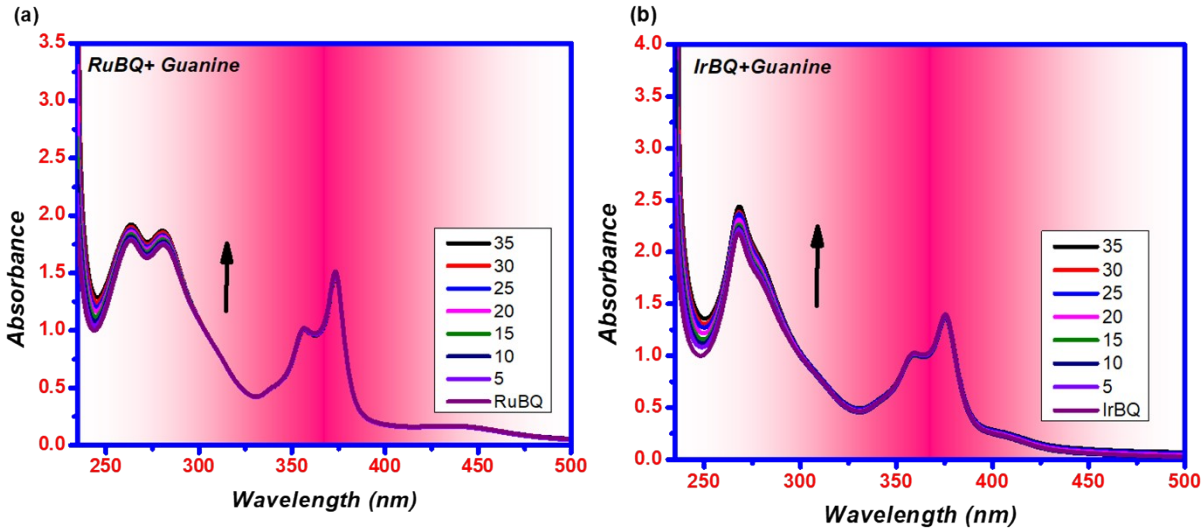

Fig. S23: Concentration dependent binding study of RuBQ and IrBQ complexes with concentration of 3 × 10^{-5} M with 1 mM Guanine.

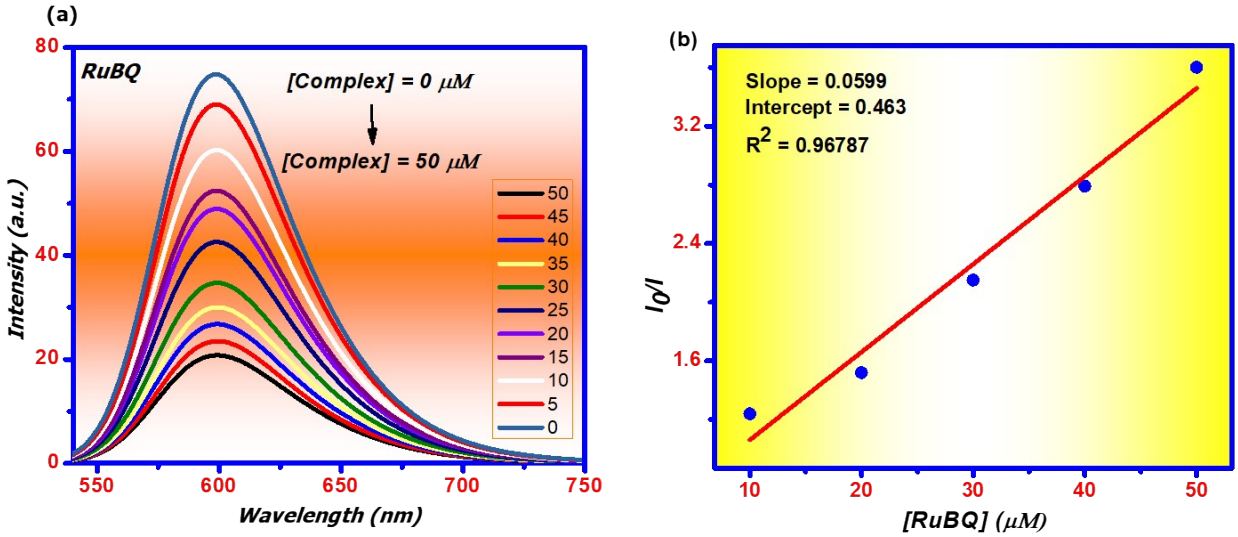

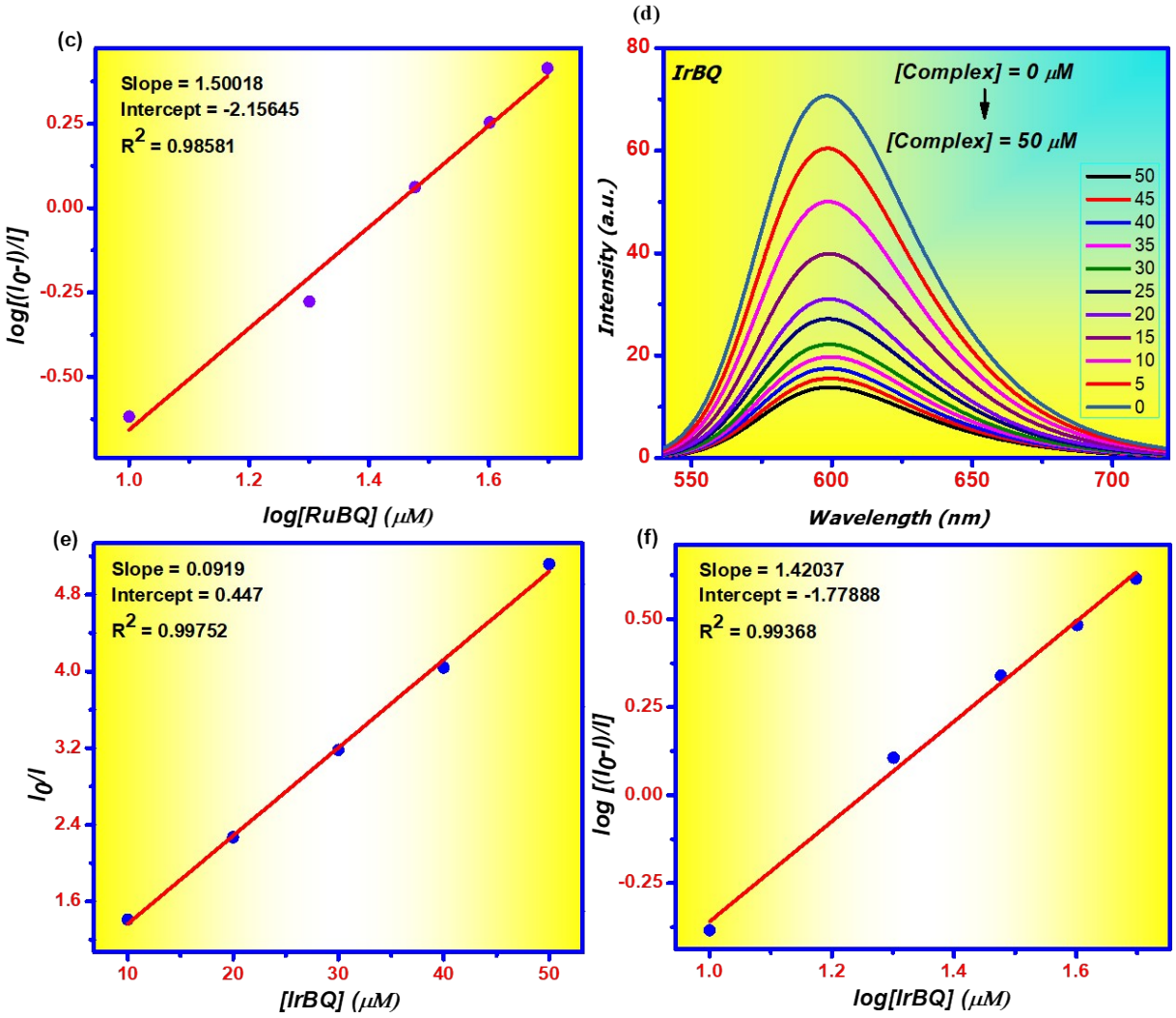

Fig. S24: Interaction of complexes (a) RuBQ, (d) IrBQ with EtBr. Stern-Volmer Plot of I_0/I vs. concentration of complexes (b) RuBQ, (e) IrBQ. Scatchard Plot of $\log[I_0-I/I]$ vs. log[Complex] for EtBr in the presence of complex (c) RuBQ, (f) IrBQ.

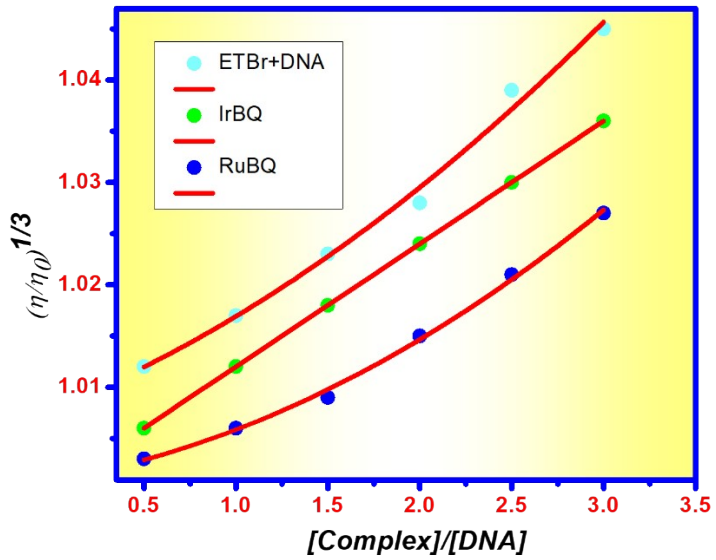

Fig. S25: Relative viscosity plot of Ct-DNA with complexes RuBQ, and IrBQ with respect to EtBr at 25 ^{0}C.

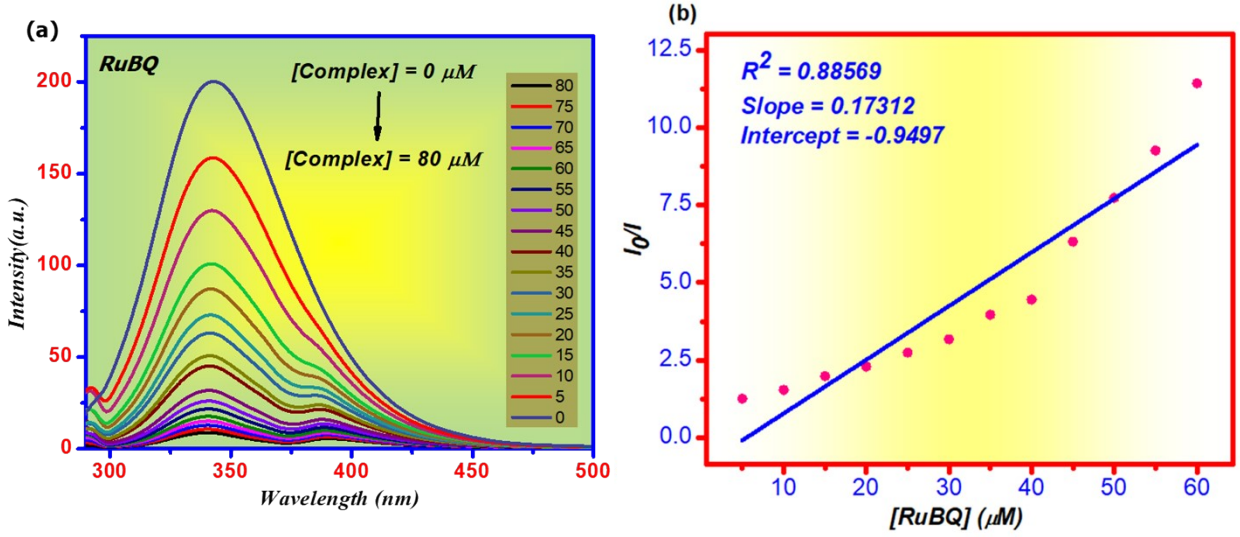

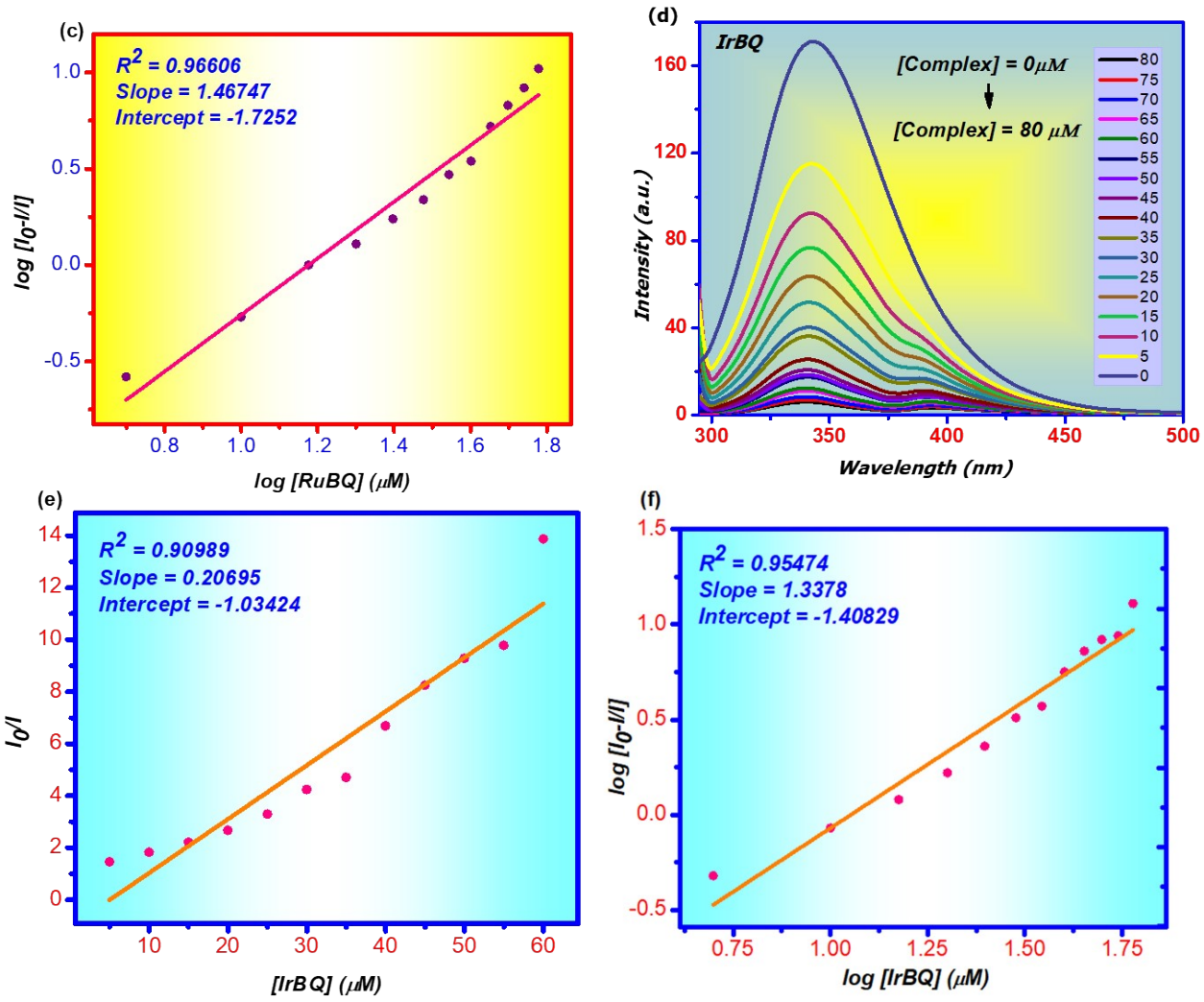

Fig. S26: Interaction of complexes (a) RuBQ, (d) IrBQ with BSA. Stern-Volmer Plot of I0/I vs. concentration of complexes (b) RuBQ, (e) IrBQ. Scatchard Plot of log[I0-I/I] vs. log[Complex] for BSA in the presence of complex (c) RuBQ, (f) IrBQ.

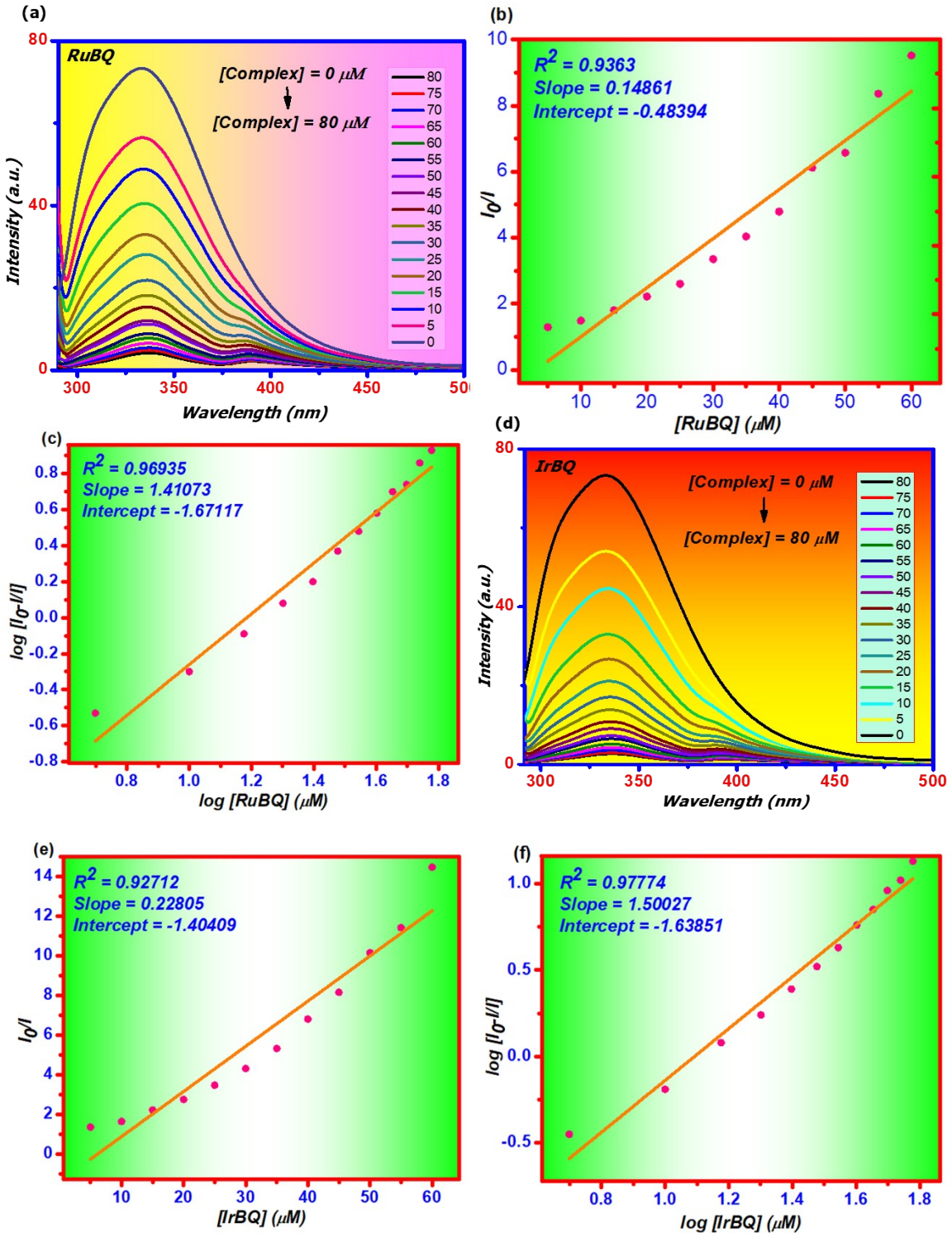

Fig. S27: Interaction of complexes (a) RuBQ, (d) IrBQ with HSA. Stern-Volmer Plot of I0/I vs. concentration of complexes (b) RuBQ, (e) IrBQ. Scatchard Plot of log[I0-I/I] vs. log[Complex] for HSA in the presence of complex (c) RuBQ, (f) IrBQ.

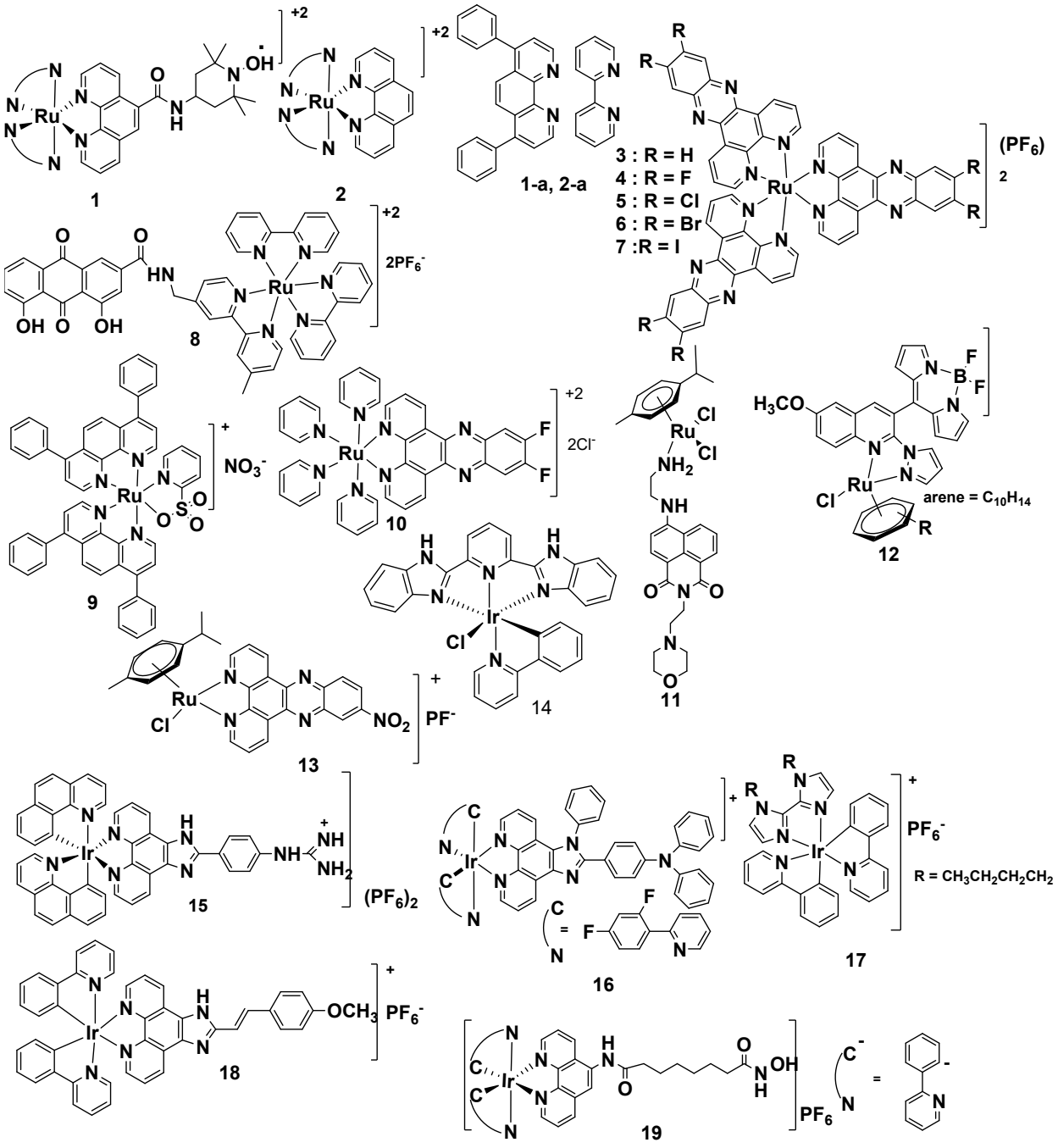

Fig. S28: Example of some Ruthenium and Iridium based PACT agent collected from literature.

Table.S1: Comparison of dark and light cytotoxicity, lipophilicity, DNA binding property between RuBQ, IrBQ and previously reported Ru and Ir based PACT agent.

Complex	HeLa cell			MCF-7 cell			Dose	Log $p_{o/w}$	DNA binding parameters (K_{app}) (10^6 M^{-1})	Ref
	Dark	Light	PI	Dark	Light	PI				
1	67.03 ± 1.5	0.24 ± 0.09	280.5	-	-	-	450 nm	-	-	31
1-a	19.2 ± 0.4	2.9 ± 0.2	6.7	-	-	-	450 nm	-	-	31
2	> 100	90.0 ± 1.6	1.1	-	-	-	450 nm	-	-	31
2-a	> 100	> 100	1.1	-	-	-	450 nm	-	-	31
3	> 100	2.12 ± 0.11	> 47	-	-	-	420 nm	1.8 ± 0.01	-	32
4	> 100	5.45 ± 0.35	> 18	-	-	-	420 nm	2.27 ±0.09	-	32
5	> 100	55.40 ±8.4	> 1.8	-	-	-	420 nm	3.29 ± 0.04	-	32
6	> 100	98.01 ± 1.9	> 1.0	-	-	-	420 nm	3.34 ± 0.20	-	32
7	> 100	> 100	-	-	-	-	420 nm	3.56 ± 0.08	-	32
8	-	-	-	250.6 ± 0.2	8.1 ± 0.3	20.9	450 nm	-0.17	-	33
9	24.6 ± 2.1	0.25 ± 0.01	56.4 ± 7.2	-	-	-	470 nm	1.10 ± 0.04	5.52 ± 0.43	34
10	> 200	8.1 ± 0.5	-	-	-	-	470 nm	-1.15 ± 0.05	6.00	35
11	31.3 ± 4.5	11.5 ± 2.5	2.71	67.2 ± 19.2	16.7 ± 1.9	4.02	448 nm	-0.06	5.04	36
12	> 100	12.87	-	-	-	-	400-700 nm	0.69 ± 0.02	6.8	37
13	13.20 ±1.52	7.53 ±0.74	-	10.76 ± 0.48	4.88 ± 1.27	-	500 nm	0.11	2.0	11
14	120.4 ± 5.4	9.5 ± 1.3	12.7	> 200	5.6 ± 0.1	> 35.7	425 nm	0.51	-	38
15	58.67 ± 1.31	0.33 ± 0.02	177.8	66.08 ± 0.84	0.71 ± 0.01	93.1	425 nm	-0.21	-	39
16	30.3 ± 1.2	0.40 ± 0.06	75	-	-	-	405 nm	1.42	-	40

17	22.5 ± 0.9	0.15 ± 0.01	150	-	-	-	405 nm	1.91	-	41
18	-	-	-	164 ± 10.3	4.31 ± 0.27 (O.P)	38.1	450 nm	-	-	42
18	-	-	-	164 ± 10.3	2.84 ± 0.14 (T.P)	57.7	800 nm	-	-	42
19	58.9 ± 3.3	3.4 ± 0.3	17.3	-	-	-	365 nm	-	-	43
19	58.9 ± 3.3	6.8 ± 0.9	8.7	-	-	-	425 nm	-	-	43
RuBQ	24.12 ± 0.62	10.48 ± 0.76	2.30	20.12 ± 0.58	9.45 ± 0.58	2.12	500 nm	0.15	2.0	
IrBQ	17.15 ± 1.46	7.23 ± 0.79	2.37	19.19 ± 0.43	8.75 ±0.46	2.19	500 nm	0.20	2.28	

O.P = One photon excitation, T.P = Two photon excitation.

Experimental Section:

UV and Fluorescence study:

Two complexes (RuBQ, IrBQ,) were evaluated using UV and fluorescence spectroscopy in 10% DMSO solution. Quantum yields of luminescence (Φ) were then determined using a 10% DMSO solution and a well-characterized standard with a known quantum yield value (William's method). Quinine sulphate was utilized as a standard. For the objective of figuring out quantum yield, the following equation (i) was used.

$$\Phi = \Phi_R \times I_S/I_R \times OD_R/OD_S \times \eta_S/\eta_R \text{ ……(i)}$$

Where, Φ = quantum yield, OD = absorbance at λ_{max}, η = refractive index of solvent(S), reference (R), I = peak area.

n-Octanol-water partition coefficient (log $P_{o/w}$):

By following the published protocol, the log $P_{o/w}$ of these complexes was calculated using the shake flask method. We used an orbital shaker to mix a known quantity of each compound with water (pre-saturated with n-octanol) for 48 hours. The solution was centrifuged at 3000 rpm for 10 minutes in order to separate its phases. Following the bilayer separation, UV-Vis spectroscopic investigation was carried out and with the help of the OD of the complexes in water and octanol, we were able to determine the partition coefficient values (log $P_{o/w}$).

Conductivity measurement:

Due to the verification of the interaction of the complexes with DMSO, aqueous DMSO, GSH, and Ct-DNA solutions, the conductivity of the complexes was measured using a conductivity-TDS meter-307 (Systronics, India) and a cell constant of 1.0 cm^{-1}. Here, we conducted the experiment at a complex concentration of 3×10^{-5} M.

Stability study:

Three complexes (RuBQ, IrBQ) were investigated for stability in several environments, including aqueous DMSO (H_2O: DMSO = 9:1), GSH medium, and PBS buffer, Cysteine medium.

Biology:

DNA binding study:

The binding efficiency of the complexes with calf thymus DNA (CT-DNA) was investigated using electronic absorption spectroscopy and competitive binding experiment was performed using fluorescence spectroscopy and EtBr as a quencher.

UV–visible studies

DNA binding study was performed with the help of complex **RuBQ**, **IrBQ** in Tris-HCl buffer (5 mM Tris-HCl in water, pH 7.4) in aqueous medium. Using it's known molar absorption coefficient value of 6600 M^{-1} cm^{-1} and its absorbance intensity at 260 nm, the concentration of CT-DNA was determined. Titration was performed by raised the concentration of CT-DNA. Before each measurement, a sample was allowed to equilibrate with CT-DNA for around 5 minutes, and then the absorbance of the resulting complex was recorded. K_b, the intrinsic DNA binding constant, was determined by using equation (ii).

$$\frac{[DNA]}{(\varepsilon_a - \varepsilon_f)} = \frac{[DNA]}{(\varepsilon_b - \varepsilon_f)} + \frac{1}{K_b(\varepsilon_a - \varepsilon_f)} \quad \text{.....(ii)}$$

Where, [DNA] = concentration of DNA in the base pairs, ε_a = apparent extinction coefficient observed for the complex, ε_f = extinction coefficient of the complex in its free form, ε_b =

extinction coefficient of the complex when fully bound to DNA. From the resulting data we got [DNA] / (ε_a-ε_f) vs [DNA] linear plot with the help of Origin Lab, version 8.5. From the ratio of slope and intercept we got the intrinsic binding constants (K_b).

Ethidium bromide displacement assay

To demonstrate the type of DNA binding occurring of the complexes, an ethidium bromide (EtBr) displacement experiment was performed. Using ethidium bromide (EtBr) as a spectral probe in 5 mM Tris-HCl buffer (pH 7.4), the apparent binding constant (K_{app}) of all the complexes to CT-DNA was determined. As the fluorescence is quenched by the solvent molecules free EtBr do not show any fluorescence. However, the intercalative method of binding of EtBr with DNA grooves was suggested by the fact that its fluorescence intensity increased radially with increasing concentrations of CT-DNA. As the complex concentrations were increased, it was observed that the fluorescence intensity decreased. In accordance with the displacement idea, the complexes are thought to have first displaced EtBr from CT-DNA grooves before binding to the DNA base pairs. Apparent binding constant (K_{app}) values were calculated using the following equation (iii).

$$K_{app} \times [\text{Complex}]_{50} = K_{EtBr} \times [\text{EtBr}] \ldots\ldots\ldots\ldots \text{(iii)}$$

Where K_{EtBr} is the EtBr binding constant (K_{EtBr} = 1.0 × 10^7 M^{-1}), and [EtBr] = 8 × 10^{-6} M. With the help of Stern-Volmer equation we determined the Stern-Volmer quenching constant (K_{SV}). We obtain linear plot of I_0/I vs. [complex] with the help of Origin 8.5 software. The value of K_{SV} was calculated from the following equation:

$$I_0/I = 1 + K_{SV}[Q]L \; L \cdots\cdots\cdots (iv)$$

Where, I_0 = fluorescence intensity in absence of complex and I = fluorescence intensities in presence of complex of concentration [Q].

Protein binding studies

Blood plasma proteins, specifically serum albumin, play crucial roles in drug delivery. We studied the interaction of the complexes with human serum albumin (HSA), and Bovine serum albumin (BSA). At the concentration of 2 x 10^{-6} M BSA and HSA solution was prepared in Tris-

HCl/NaCl buffer. The complexes' aqueous solutions were then added to the HSA and BSA solution in a stepwise fashion to raise the concentration. After each addition, the solutions were gently agitated for 5 minutes before recording the fluorescence at a wavelength of 280 nm for HSA and 295 nm for BSA. It was noticed that the fluorescence intensity gradually decreased with increasing complex concentration, proving that interaction between the complex and HSA or BSA occurred. With the help of Stern-Volmer equation we quantitatively determine the quenching constant (K_{BSA}). We obtained linear plot of I_0/I vs. [complex] using the equation (v) with the help of Origin Lab, version 8.5.

$$I_0/I = 1 + K_{BSA/HSA}[Q] = 1 + k_q \tau_0[Q]L\ L \cdots\cdots\cdots(v)$$

Where I_0 = the fluorescence intensity of BSA/HSA in absence of complex, I = the fluorescence intensity of BSA/HSA in presence of complex of concentration [Q], τ_0 = lifetime of the tryptophan in BSA/HSA found as 1×10^{-8}, k_q = the quenching constant. Equation (vi) gives the binding properties of the complexes.

$$\log(I_0 - I/I) = \log K + n \log [Q]L\ L \cdots\cdots\cdots(vi)$$

Where, K = binding constant, n = number of binding sites.

Singlet oxygen (1O2) quantum yield determination

Using visible light (400-700 nm) for photosensitization, the singlet oxygen ($^1O_2$) quantum yields of complexes in DMSO at room temperature were calculated. In order to calculate the $^1O_2$ quantum yields we observed the photooxidation of DPBF after sensitization by the complex. From 10 s to 140 s, DPBF photooxidation was recorded. Quantum yield of $^1O_2$ was determined by using Rose Bengal (RB) ($\Phi[^1O_2]$ 0.76 in DMSO) as a reference molecule and comparing the quantum yield of DPBF photooxidation after sensitization by the compound of interest to that of RB using Equation (vii).

$$\Phi\Delta_c = \Phi\Delta_{RB} \times m_c/m_{RB} \times F_{RB}/F_C \ldots\ldots\ldots\ldots\ldots\ldots(Vii)$$

where c = complex, and RB = Rose Bengal. $\phi\Delta = {}^1O_2$ quantum yield, and m is the slope of the plot of DPBF absorbance at 417 nm vs. irradiation time. F = absorption correction factor, which is given by Equation (viii).

$$F = 1\text{-}10^{OD} \quad \text{..... (viii)}$$

Where, OD is the optical density at the irradiation wavelength.